Improved LJF Equations for the Uni-Planar Gapped K-Type Tubular Joints of Ageing Fixed Steel Offshore Platforms

R Khan PhD, CEng CMarEng FIMarEST FIET, FICE**; K Smith** MSc, CEng, MICE

I Kraincanic PhD

London South Bank University, UK

SYNOPSIS

The distribution of fixed steel offshore platforms around the world reveals a global fleet that has exceeded or is approaching the end of the design life of the facility. In many operating areas, there is an attraction to continue using these ageing facilities due to continued production or as an adjoining structure to facilitate a new field development or expansion. To justify continued life extension of the fixed platform, various integrity assessment techniques are often used. One of the major techniques used is based on the phenomenon of Local Joint Flexibility (LJF).

While the phenomenon of LJF has been well known in the offshore industry since the early 1980s, there has been little experimental data available. In 1983, Amoco conducted an experimental study primarily to determine stress concentration factors associated with gapped K-type steel tubular joints. The LJFs were also calculated as part of the study by using the chord and brace displacements observed of two specimens under eleven load cases. The LJFs calculated were based on the effects of in-plane bending, out-of-plane bending and axial compression and tension. Presently there are at least ten sets of LJF equations that have been used since the 1980s to predict fatigue life estimation and ultimate strength of the jacket structures. Their derivations have evolved in many ways including use of finite element methods to predict the joint behavior. There has been no benchmarking exercise to large-scale experimental data.

This paper provides an improvement on existing LJF equations by benchmarking the Amoco K-joints test results to a finite element model and through a detailed parametric study. Improved formulations are provided for local joint flexibilities for gapped uni-planar K-type tubular steel joints.

Authors' Biographies

Dr Riaz Khan is a chartered engineer with over twenty years of experience in the civil engineering discipline. He has particular expertise in the structural integrity management of fixed and floating offshore structures and has assumed responsible positions on a variety of projects ranging from major offshore and onshore field developments. He has developed particular skills in the area of life-cycle integrity management for energy related. His experience also includes conceptual field development studies, detailed design and analyses of both onshore and offshore structures including fatigue, seismic, vessel impact, decommissioning and ultimate strength considerations in a variety of operating regions including the Gulf of Mexico, North Sea, Latin America, Asia and the Far East. He also serves as a Task Group Leader and Member of the OGP (ISO 19901-9) Code Committee for the Structural Integrity Management of Fixed Offshore Structures.

Kenneth Smith is a Reader of Structural Engineering at the London South Bank University and a chartered civil engineer. He has over thirty years of both industry and lecturing experience with his research interests including forensic engineering and conservation, asset integrity management and structural engineering.

Dr Ivana Kraincanic is a Senior Lecturer at the London South Bank University who specialises in finite element analysis, dynamic analysis and earthquake engineering. Her research interest also covers diverse topics of steel cables, offshore flexible pipelines, reinforced concrete slabs, and steel fibre-reinforced concrete.

ABBREVIATIONS

ABAQUS	ABAQUS Suite of Finite Element Analysis Software
AMOCO	American Oil Corporation
API	American Petroleum Institute
ASAS	Atkins Structural Analysis System
BOMEL	Billington Osbourne Moss Engineering Limited
BP	British Petroleum
DNV	Det Norske Veritas
FEM	Finite element methods
GoM	Gulf of Mexico
HSE	Health, Safety and Environment
IPB	In-Plane Bending
ISO	International Standards Organization
JIP	Joint Industry Project
LJF	Local Joint Flexibility
LSBU	London South Bank University
MSL	MSL Engineering Corporation
OGP	Oil and Gas Producer
OPB	Out -of- Plane Bending
OTC	Offshore Technological Conference (Houston)
RBI	Risk Based Inspection
RLA	Remaining Life Assessment
RP	Recommended Practice
UEG	Underwater Engineering Group (UK)
USFOS	Ultimate Strength Finite Element Software
Wimpey	Wimpey Laboratories Limited

SYMBOLS

D	Chord diameter
d	Brace diameter
R	Chord radius
δ	Axial displacement of the brace
δ_F	Displacement attributable to joint flexibility
E	Young's Modulus of Elasticity
F	Axial force
f_{kj}	Flexibility matrix terms
T	Chord Thickness
t	Brace thickness
ϕ	Angle between brace and x-z plane (degrees)
θ	Angle between the brace and the x- axis
K	Joint stiffness coefficient
L	Chord length
M	Bending moment
g_l	Longitudinal gap length
g_t	Transverse gap length
λ	Cross sectional area of the brace
τ	Brace to chord wall thickness ratio
β	Brace to chord diameter ratio
α	Chord length to chord radius ratio
γ	Radius to wall thickness ratio of the chord
ζ	Gap parameter for K joint

1.0 INTRODUCTION

The vintage of fixed offshore steel structures globally range from those installed in the 1950s to those designed to the latest code of practice [2,16]. A great variety of the grandfather type structures are still operating well beyond their design life and leading the industry to believe they are still fit for purpose with regards to fatigue lives and ultimate strength. Figure 1 shows that as of 2005, 48% (1947 of 4024) of the fixed offshore structures currently operating in the Gulf of Mexico have exceeded their design life (of 25 years). Interestingly, another 40% have reached the end of their design life by 2015.

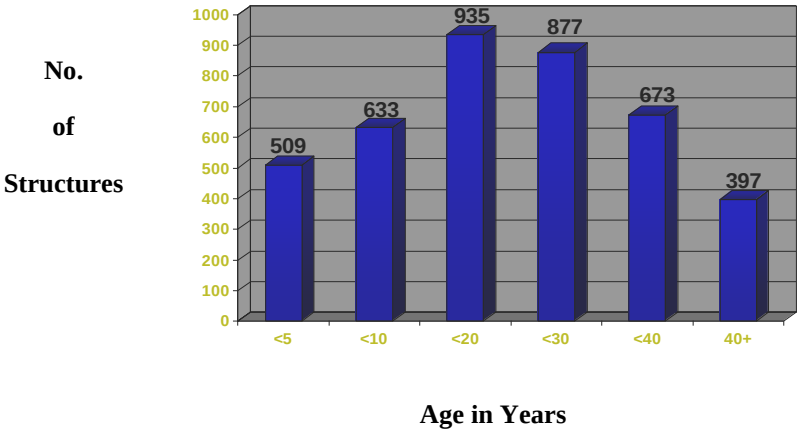

Figure 1 Platform lives in the Gulf of Mexico [21]

Nichols et al. (2006) [16] also identified a similar trend in the ageing of offshore facilities in Malaysian waters. They provided the following table as evidence of an ageing fleet for three operating regions in Malaysia. Table 1 indicates that of the 165 offshore structures operating by a major operator (as of 2006), approximately 44% are operating beyond 25 years and approximately 24 % were operating beyond 30 years.

	Age Distribution, *x* (Years)				
	***x*<10**	**10<*x*<20**	**20<*x*<25**	**25<*x*<30**	***x*>30**
Region A	13	5	13	4	
Region B	1	3	7	10	6
Region C	1	33	17	19	33

Table 1 Platform Profile, 2006 in major operator in South East Asia – Age Distribution [19]

MSL Engineering in 2001, on behalf of the UK Health and Safety Executive, undertook the study *The effects of local joint flexibility on the reliability of fatigue life estimates and inspection planning* [11]. The findings of this study supported the industry view that conventional rigid joint analysis under-predicts fatigue life, while implementing local joint flexibility allows for a more accurate fatigue life prediction and closer agreement with results from underwater inspection and results in reducing the requirement for costly underwater inspections by approximately 75%. It is through studies such as these that the benefits of local joint flexibility can be realized and they provide a basis for further research on local joint flexibility, Oil and Gas Producers (OGPs) are faced with fitness for purpose engineering evaluations for an ageing global fleet.

2.0 AMOCO K-JOINT TESTS

In 1983, AMOCO conducted an experimental study primarily to determine stress concentration factors associated with gapped K-type steel tubular joints [17]. The LJFs were also calculated as part of the study by using the chord and brace displacements observed on two specimens under eleven load cases. The LJFs calculated were based on the effects of in-plane bending, out-of-plane bending, and axial compression and tension. The objective of the tests was to determine the ultimate strength of the joints in the as-welded condition, under static loading, for comparison with

strengths predicted by existing design codes and parametric equations. In addition, stress concentration factors and local joint flexibilities, under elastic loading, were determined for the as-welded condition.

The joints of tested were:

- Of the non-overlapping K configuration and consist of 18 inch (457 mm) outer diameter (OD) chords and 16 inch (406 mm) outer diameter (OD) braces.
- The chord wall thicknesses are either 0.394 inch (10 mm) or 0.375 inch (9.5mm) and the brace thickness is 0.394 inch (10 mm).
- The angles of intersection vary but are, typically, in the range of 40 to 60 degrees. It was Amoco's intention that the tests should be carried out on the heavily loaded K joint which is that one with an intersection angle of 60◦ between the chord and the braces.

The geometry of this joint is given in Figure 2 and the loadings in Figure 4. *The experimental data presented [15] are the only published large scale test data on LJF.*

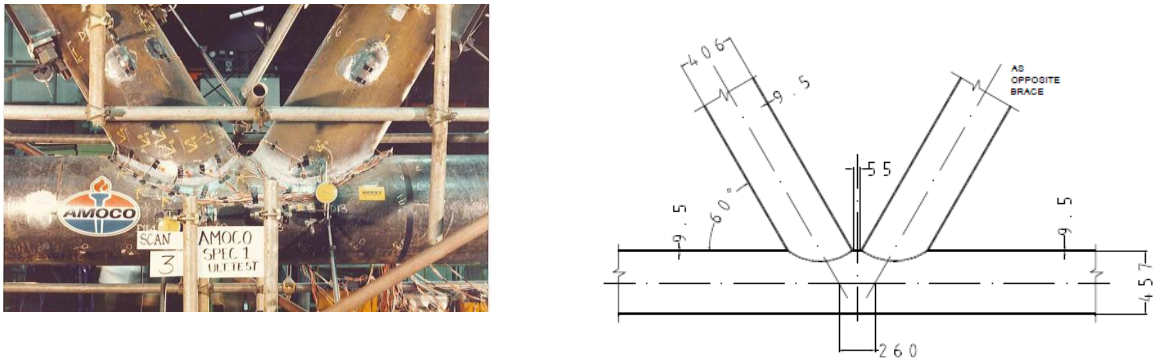

Figure 2 AMOCO K-Joint [17]

The geometrical parameters for the AMOCO K-Joints include $\beta = d/D = 0.89$, $\gamma = R/T = 24$, $\zeta = g/D = 0.12$, $40^{\circ} \leq \theta \leq 60^{\circ}$. Local joint flexibility measurements were made for the eleven (11) load cases shown in Figure 4. Previous to this study [15], there were no large scale test results for K joints. The measured and predicted values for local joint flexibility under axial load, in-plane and out-of-plane bending are shown in Table 2.

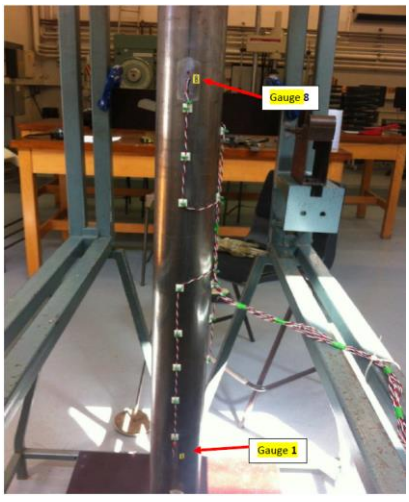

Figure 3 LSBU small scale tests [7]

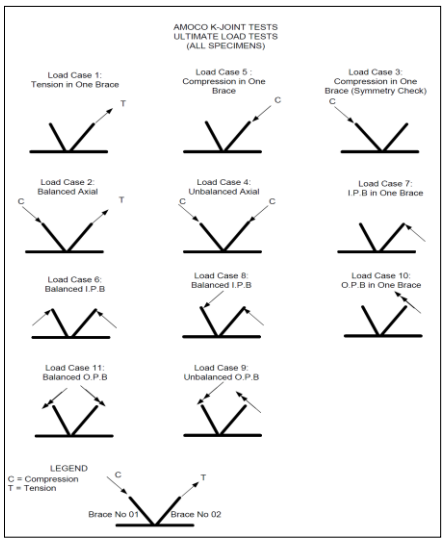

Figure 4 Loadings on Specimens 1 & 2, Amoco K Joint Tests

In 2015, LSBU conducted LJF tests on a small scale model to address IPB condition [7]. The testing of the in-plane condition was selected on the basis that the major source of ambiguity in the AMOCO K-Joint tests was in the comparison of the in-plane condition experimental results and the finite element results. It should be noted that a scaling factor of ¼ the size of the dimensions of the large scale specimen was used which is deemed acceptable, as a rule of thumb in the preparation of small scale models. The main source of difficulty in measuring IPB stems from an inability to appropriately position the transducers at the brace and chord to simulate the chord distortion, especially when ultimate capacity has been achieved, but more importantly for the LSBU tests, is that they were able to show similar deformed shape to that of the Amoco K-Joints for IPB. This was quite useful as it indicated consistency between both tests in terms of their modes of failure.

Load Case	Brace 1	Brace 2	
	Local Joint Flexibility	Local Joint Flexibility	Units
1- Axial	1.7	3.8	$x10^{-3}$ mm/kN
2- Axial	-1.2	1.4	$x10^{-3}$ mm/kN
3- Axial	2.6	2.5	$x10^{-3}$ mm/kN
4- Axial	8.4	6.7	$x10^{-3}$ mm/kN
5- Axial	1.6	3.9	$x10^{-3}$ mm/kN
6- In Plane Bending	2.7	2.3	$x10^{-5}$rad/kNm
7- In Plane Bending	0.8	3.7	$x10^{-5}$rad/kNm
8- In Plane Bending	4.1	4.9	$x10^{-5}$rad/kNm
9-Out of Plane Bending	17.4	16.3	$x10^{-5}$rad/kNm
10- Out of Plane Bending	11.2	12.1	$x10^{-5}$rad/kNm
11- Out of Plane Bending	26.3	3.0	$x10^{-5}$rad/kNm

Table 2 Local Joint Flexibility for Specimen 1, (Amoco K-Joint Test Results 1983) [17]

3.0 EXISTING PARAMETRIC FORMULATIONS ON LJF

Presently there are ten published sets of LJF equations that have been used since the 1980s to predict fatigue life and ultimate strength of the jacket structures. There derivations have evolved in many ways including use of finite element methods to predict the joint behaviour. There has been no benchmarking exercise to large scale experiment. The details of the existing LJF formulations are provided in Table 3.

No.	Year of Study	Researcher	Research/Study
1	1977	**Det Norske Veritas (DNV) [9]**	Proposed formulae for the translational and rotational spring stiffness for T joints within the DNV (1977) "Design, Construction and Inspection of Offshore Structures"
2	1983 & 1986	**Fessler et al. at Nottingham University [13,14]**	Published a set of LJF formulae for T/Y joints based on tests on precision-cast epoxy specimens. The formulae have been updated in 1986 and are generally referred to as the Fessler improved equations. Formulations have now been adopted within the SACS Software.
3	1985	**Efthymiou [12]**	Produced a series of LJF expressions for the bending load cases.
4	1987	**Ueda et al. [24]**	Published LJF equations for 90 degree T joints under axial load and in-plane bending.

5	1993	**Hoshyari and Kohoutek [15]**	Published expressions for the flexibility of tubular T joints studied using a dynamic method of analysis.
6	1993	**Chen et al. [6]**	Modified the earlier work on the semi-analytical method to account for T/Y, K symmetric and K non-symmetric joints and extended the work to cater for multi planar braces.
7	1993	**Butraigo et al. [5]**	Developed LJF parametric equations which showed a string dependency on the β and γ with a lesser influence on the τ and θ parameters. Formulations have now been adopted within the SACS software.
8	2002	**MSL-Joint [8]**	Developed as a part of JIP for ultimate strength, the formulations are now adopted within the SACS and USFOS Software.
9	2013	**Qian et al. [22]**	Attempted to benchmark current research at National University Singapore to MSL equations and BOMEL Frame Tests.
10	2014	**Asgarian et al. [3]**	An FE based study of single planar multi-brace tubular Y-T and K-Joints.

Table 3 Existing LJF parametric equations used in the offshore structural industry

4.0 LJF BENCHMARKING STUDY

Prior to the Benchmarking Study, a mesh size and refinement study was performed which shows that the 4-Noded General Purpose Shell Element (S4R) in ABAQUS [1] would yield convergent displacement results, close to those obtained from the experimental study (Table 4). The use of shell type elements has the added advantage, of not having to model the weld profile and details, as per the recommendations provided in DNV RP 203(2010) [10]. The FE analysis focused on obtaining displacement values, which is the primary result required to predict LJF. Unlike FE stress concentration models which are generally sensitive to mesh refinement and element type, FE displacement models are not as sensitive to element type and mesh refinement, provided the FE mesh generated, is reasonably refined. The Mesh Generator in ABAQUS serves as a building model tool and is used in this study instead of manual mesh generation. The results of the FE analysis were compared to test data provided in the AMOCO test joint for Local Joint Flexibility for axial compression, tension and out-of-plane and in-plane bending.

Load	AMOCO K-Test Results	FE Results Refined Mesh	% Difference
Total Displacement (Axial)- Load Case 2- Tension Brace only	**0.0031** (mm/kN)	**0.0028** (mm/kN)	9.67%
Total Displacement (Out -of-plane Bending)- Load Case No 11, Brace 1 only	**3.90 E-05** (rad/kN-m)	**3.917 E-05** (rad/kN-m)	0.43%
Total Displacement (In-plane Bending)- Load Case No 06, Brace 1 only	**3.21 E-05** (rad/kN-m)	**3.164 E-05** (rad/kN-m)	1.43%

Table 4 Mesh Sensitivity results

The finite element (FE) models with eleven load cases (from Figure 4) were created in ABAQUS to represent the geometry and loadings of the specimens (Figure 4). The main objective of the FE model generation was to benchmark the AMOCO Test Data by providing a finite element gapped K-joint model that best represents the results of the eleven load cases. FE models for Load Case 10 are shown in Figure 5.

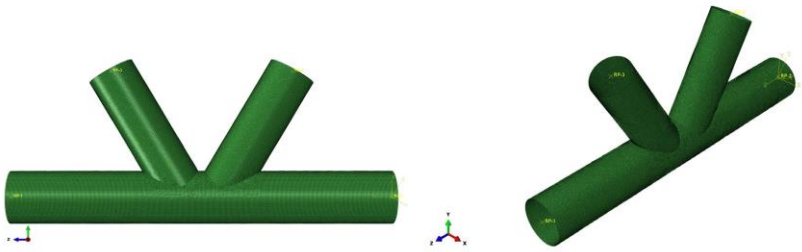

Figure 5 AMOCO K Joint Finite Element Benchmark Model, Y-Z and X-Y-Z plane view (ABAQUS for Load Case 10)

The chord walls at the supports in the FE model were restrained from translation in the x and y directions to maintain the roundness of the chord section. The joint is modeled as part of a structure where the beam theory is no longer valid and must be replaced by shell theory, to derive the benefits of the FE model. In the FE model, the end cross sections behave as rigid planes with no "ovalization" (Figure 6). The contribution made by chord rotations are calculated on spreadsheets and added to the overall LJF of the joint. The methodology for determining the LJF are provided on Figure 7.

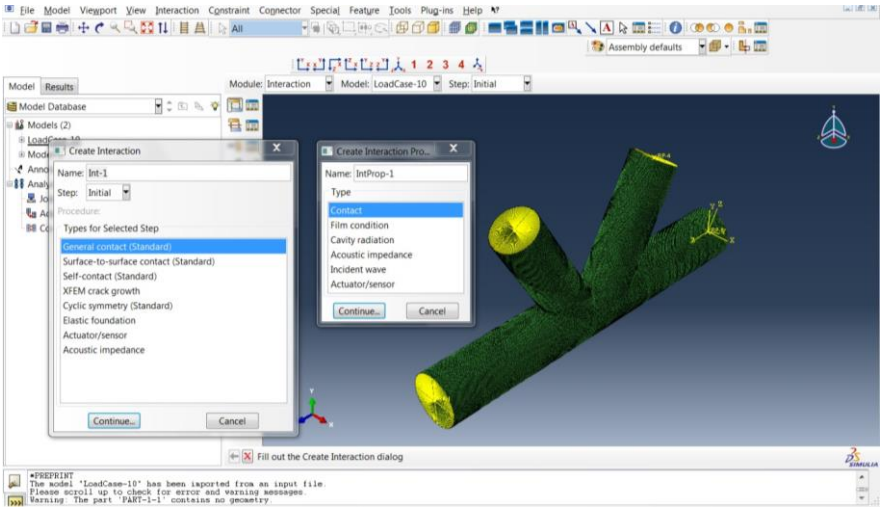

Figure 6 AMOCO K-Joint Finite Element Benchmark Model, Creating Load Step and Boundary Conditions (generated in ABAQUS 6.11)

The calculated values for LJF at each of the braces and the related flexibility coefficients are provided within Table 5 and based on the procedure outlined in Figure 7.

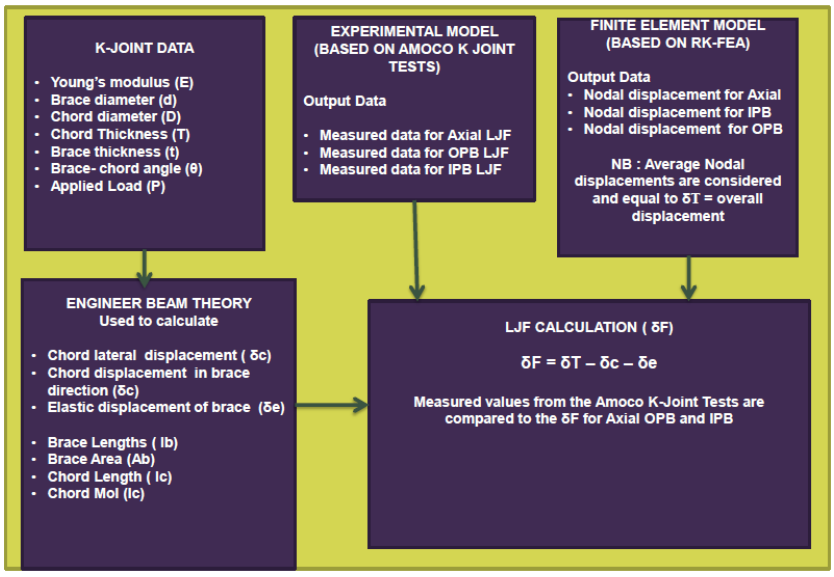

Figure 7 Procedure for the calculation of LJF for Axial, OPB and IPB

$$\begin{bmatrix} \delta_1 \\ \Phi_{o1} \\ \Phi_{i1} \\ \delta_2 \\ \Phi_{o2} \\ \Phi_{i2} \end{bmatrix} = \begin{bmatrix} f_{11} & & & f_{14} & & \\ & f_{22} & & & f_{25} & \\ & & f_{33} & & & f_{36} \\ f_{41} & & & f_{44} & & \\ & f_{52} & & & f_{55} & \\ & & f_{63} & & & f_{66} \end{bmatrix} \times \begin{bmatrix} P_1 \\ M_{o1} \\ M_{i1} \\ P_2 \\ M_{o2} \\ M_{i2} \end{bmatrix}$$

Figure 8 Flexibility Coefficients in the Matrix Form

		RK Finite Element Analysis	Measured (AMOCO K-Joint Tests)	Units
f_{11}=	f_{44}=	**3.2**	**3.8**	x10^{-3} mm/kN
f_{14}=	f_{41}=	**1.6**	**1.7**	x10^{-3} mm/kN
f_{22}=	f_{55}=	**11.2**	**12.1**	x10^{-5}rad/kNm
f_{25}=	f_{52}=	**7.4**	**11.2**	x10^{-5}rad/kNm
f_{33}=	f_{66}=	**3.0**	**3.7**	x10^{-5}rad/kNm
f_{36}=	f_{63}=	**0.3**	**0.8**	x10^{-5}rad/kNm

Table 5 Flexibility Matrix Coefficients from AMOCO K-Joint Tests and FE Modeling

5.0 LJF COMPARISON STUDY FOR AMOCO K JOINT GEOMETRY

The existing formulations applicable to single-planar gapped K-type joints are the Fessler, Efthymiou, Chen, Butraigo, Asgarian and MSL equations. However, Efthymiou's equations are only applicable for in-plane and out-of plane bending. MSL-Joint formulations are not considered in the comparison study, as joint flexibility is considered as implicit to the MSL equation for ultimate strength.

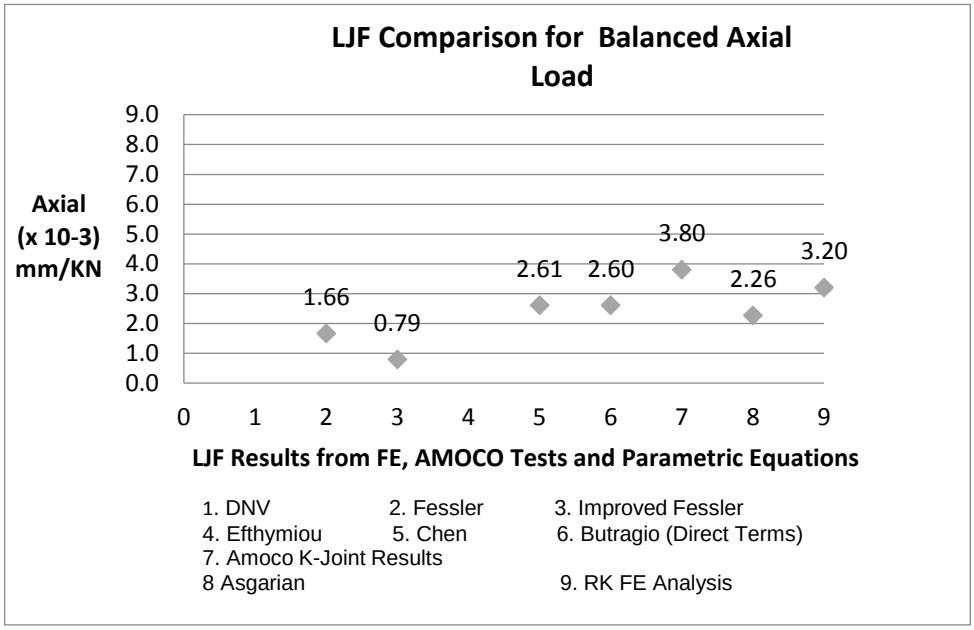

Figure 9 LJF Comparison for Axial Loading (Direct Terms)

For axial loading (Figure 9) the results from the direct terms associated with the RK FE modeling and the AMOCO K Joint tests are within 20% of each other,. Improved Fessler's equations under predicts LJF by approximately 80%. Fessler's equations under predicts LJF by approximately 60% and Butraigo and Chen under predict 30% compared to the K-joint test results.

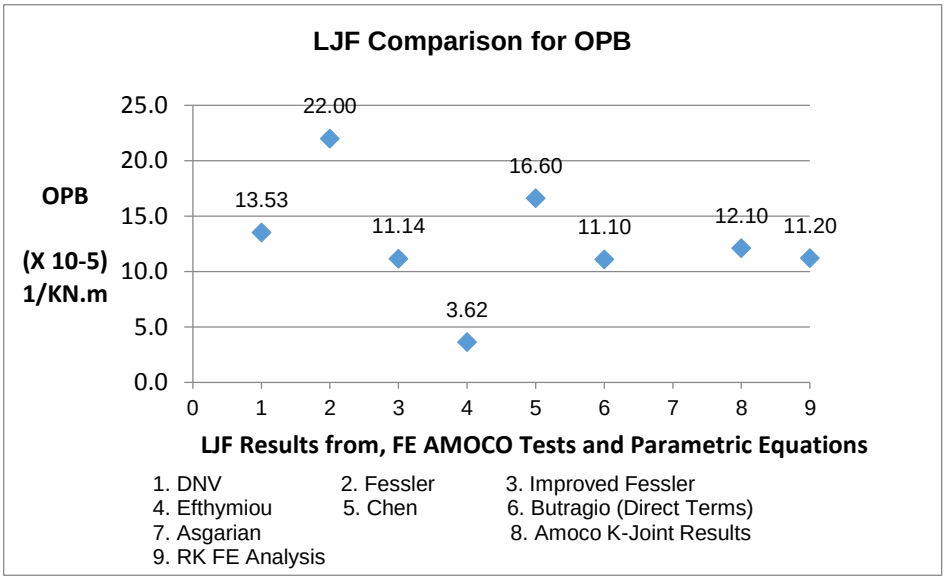

Figure 10 LJF Comparison for Out of Plane Bending

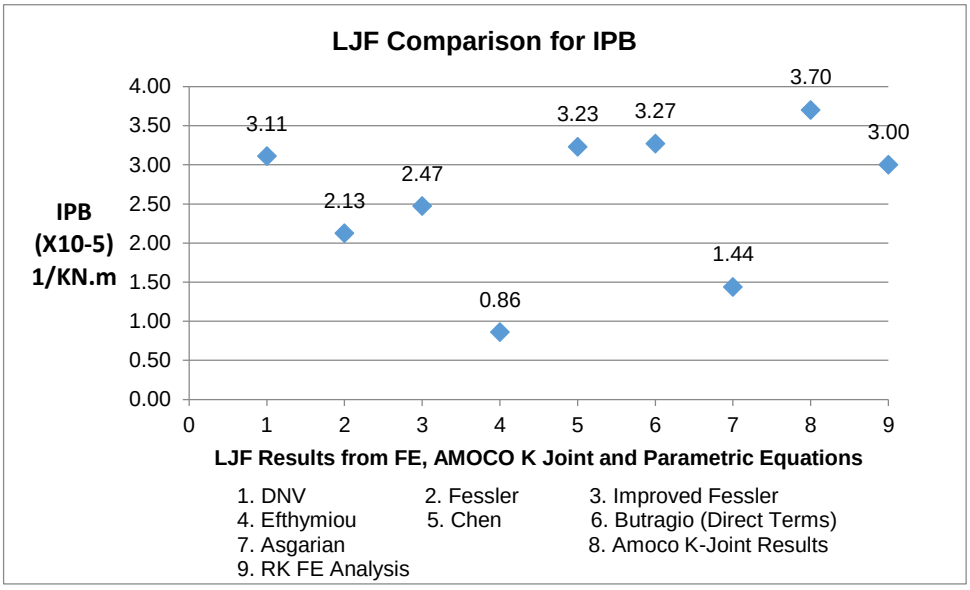

Figure 11 LJF Comparison for In Plane Bending

For OPB Improved Fessler, Buitrago, FE modeling are within 10% of the K-joint test results (Figure 10). Efthymiou's equations under-predict the LJF by 73% and Asgarian do not consider out of plane bending. While DNV, Fessler and Chen over-predicts LJF for out-of plane bending by 20%, 42% and 13% respectively. For IPB (Figure 11), DNV, Chen, Buitrago and RK-FEA results are within 20% of the AMOCO Test results. Efthymiou's equations under-predict by 77%, Asgarian by 61% and, Fessler and Improved Fessler's equations under predict in the range of 30-45%. From Table 7 the RK-FEA benchmark model consistently provides results are similar to the AMOCO K-joint tests. The main conclusion that can be deduced from the benchmarking and comparison studies is that the RK-FEA benchmarking finite element model produces flexibilities within 10-20% for axial and in-plane bending and within 10% for out-of-plane bending compared to the test results and thus can be used to develop more elaborate parametric LJF equations for single-planar gapped K-joints. The other LJF formulations consistently produce results that are well over 30% (either over predicting or under predicting) of the measured results. A summary of the results for the LJF comparison on the AMOCO K-joint tests is provided in Table 6.

	Axial				**Out-of-Plane Bending**				**In-Plane Bending**			
	< 10%	10% - 20%	20% - 30%	> 30%	< 10%	10% - 20%	20% - 30%	> 30%	< 10%	10% -20%	20% - 30%	> 30%
RK-FEA		**X**			**X**					**X**		
DNV							**X**			**X**		
Fessler				**X**	**X**							**X**
Improved Fessler				**X**	**X**							**X**
Efthymiou								**X**				**X**
Chen				**X**						**X**		
Buitrago				**X**	**X**			**X**		**X**		
Asgarian				X								X

Table 6 LJF Comparison Study Results Summary

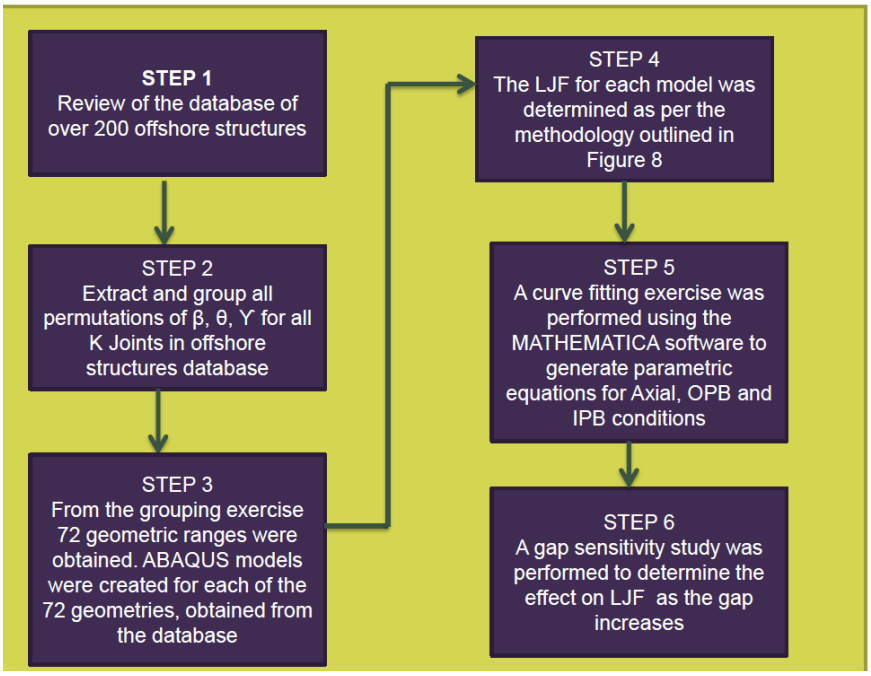

Figure 12 Six Step Work Flow Process to develop the RK-LJF Parametric Equations

Having established the methodology (Figure 7) for the calculation of the LJF from numerical methods, this methodology was used to develop a suite of parametric equations from by introducing a step-by-step process for all in-service K-type steel joints. The six step methodology is provided in Figure 12.

6.0 DATABASE OF IN-SERVICE FIXED OFFHSORE STRUCTURES

A data collection exercise was embarked upon, using an offshore structures database and associated drawings to catalogue the geometrical properties of in-service K-type joints. The structural database is used for the structural integrity management of over 200 fixed steel offshore structures in South East Asia and has been developed and maintained by a major oil and gas operator. The platforms in the structural database are of various vintages ranging from pre-API RP 2A Structures to those designed to modern API RP 2A code of practice [2,16]. From the platforms that are considered as a representative sample of existing structures, over one thousand K-type joints were recorded and compiled. A total of 38 groups of variations of β, ϒ, ζ, Gap g and Brace - Chord Angle, Θ were established for constant chord diameters. Fessler [13,14] concluded that it is very rare for tubular joints to be outside of the following ranges.

$$10 \leq \gamma \leq 20, \qquad 0.30 \leq \beta \leq 0.80, \qquad 30^{\circ} \leq \theta \leq 60^{\circ}$$

A further K-Joint data collection and screening using a Structural Integrity Management (SIM) database was undertaken to ensure that the geometric ranges proposed by Fessler [13,14] were initially considered. There are a number of K-type joints where $\gamma < 10$ and $\beta > 0.80$ so these K-joint geometric parametric ranges are included in this study in addition to Fessler's recommendations. A total of 72 K-Joint geometric ranges were considered from the platform screening and K-Joint Study that can adequately provide a full range of data points for determining improved local joint flexibility parametric equations. Table 8 provides the full set of geometric ranges used.

Geometric Range No	γ = D/2T	β = d/D	θ	Geometric Range No	γ = D/2T	β = d/D	θ	Geometric Range No	γ = D/2T	β = d/D	θ
`1	8	0.30	30	31	20	0.50	30	61	15	0.89	30
2	8	0.30	45	32	20	0.50	45	62	15	0.89	45
3	8	0.30	60	33	20	0.50	60	63	15	0.89	60
4	8	0.50	30	34	20	0.70	30	64	20	0.89	30
5	8	0.50	45	35	20	0.70	45	65	20	0.89	45
6	8	0.50	60	36	20	0.70	60	66	20	0.89	60
7	8	0.70	30	37	25	0.30	30	67	25	0.89	30
8	8	0.70	45	38	25	0.30	45	68	25	0.89	45
9	8	0.70	60	39	25	0.30	60	69	25	0.89	60
10	10	0.30	30	40	25	0.50	30	70	30	0.89	30
11	10	0.30	45	41	25	0.50	45	71	30	0.89	45
12	10	0.30	60	42	25	0.50	60	72	30	0.89	60
13	10	0.50	30	43	25	0.70	30				
14	10	0.50	45	44	25	0.70	45				
15	10	0.50	60	45	25	0.70	60				
16	10	0.70	30	46	30	0.30	30				
17	10	0.70	45	47	30	0.30	45				
18	10	0.70	60	48	30	0.30	60				
19	15	0.30	30	49	30	0.50	30				
20	15	0.30	45	50	30	0.50	45				
21	15	0.30	60	51	30	0.50	60				
22	15	0.50	30	52	30	0.70	30				
23	15	0.50	45	53	30	0.70	45				
24	15	0.50	60	54	30	0.70	60				
25	15	0.70	30	55	8	0.89	30				
26	15	0.70	45	56	8	0.89	45				
27	15	0.70	60	57	8	0.89	60				
28	20	0.30	30	58	10	0.89	30				
29	20	0.30	45	59	10	0.89	45				
30	20	0.30	60	60	10	0.89	60				

Table 7 K-Joint Geometric Ranges (input for ABAQUS Analysis)

7.0 FINITE ELEMENT MODELLING OF DATABASE OF K-TYPE JOINTS

ABAQUS Structural models are created for each of the 72 geometric ranges in Table 7. The structural models have been created based the ABAQUS Benchmarking model methodology Typical ABAQUS models varying geometric ranges are shown on Figures 10a through 10c. For each of the 72 models Axial Balanced, In-plane Bending (IPB) and Out-of-Plane Bending effects are calculated based on the Excel spread-sheet structural calculations. Five (5) Load cases were applied to each of the seventy two (72) ABAQUS models. These are provided in Table 7.

Load Case	Condition	Loading – Brace 1	Loading – Brace 2	Comments
LC1	Axial Balanced	1 KN Compression on Brace 1	1 KN Compression on Brace 2	
LC2	IPB (22)	-	1KN-m moment applied on brace 2	LJF calculated on Brace 2
LC3	OPB (22)	-	1KN-m moment applied on brace 2	LJF calculated on Brace 2
LC4	IPB (21)	-	1KN-m moment applied on brace 2	LJF calculated on Brace 1
LC5	OPB (21)	-	1KN-m moment applied on brace 2	LJF calculated on Brace 1

Table 8 Loading System for all geometric models

The 72 geometric ranges in Table 8, will be used to develop ABAQUS structural models to determine LJF for the Balanced Axial, IPB and OPB conditions using the methodology outlined in Figures 7 and 12.

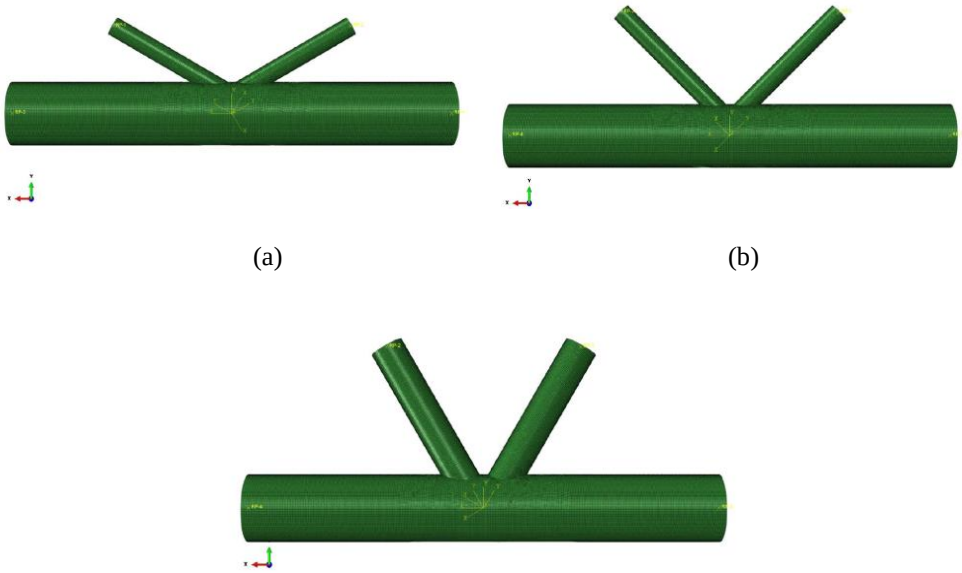

(a) (b)

(c)

Figure 13 K - Type Tubular Joint models, (a) $\beta = 0.3$, $\gamma = 10$, $\theta = 30^\circ$
(b) $\beta = 0.3$, $\gamma = 10$, $\theta = 45^\circ$
(c) $\beta = 0.5$, $\gamma = 15$, $\theta = 60^\circ$

The results of the LJF values for the loading effects due to axial balanced, IPB and OPB for β values of 0.3, 0.5, 0.7 and 0.89 are calculated using the same methodology as the benchmarking study.

8.0 DEVELOPING THE LJF PARAMETRIC EQUATIONS

The results generated from the calculations in Section 7.0 represent the performance of a full range of K-joint geometric parameters that can be used to accurately produce a suite of LJF equations for IPB, OPB and balanced axial loadings. The *Mathematica* software was used to generate the LJF parametric equations. A major scientific tool in *Mathematica* is the manifold of plotting routines that helps to depict mathematical results graphically and is a

good tool for making 3- dimensional graphs. Typically, the model will only contain a single variable while the parameters to be fit may be two or more items. The chord diameter is a constant throughout the FE analysis while the parameters include variations of β, γ and θ. The expressions generated from the *Mathematica* curve fitting is provided in the 3D plots shown in Figure 11. For Axial Balanced, IPB and OPB, the following RK LJF expressions were derived and presented in Table 9.

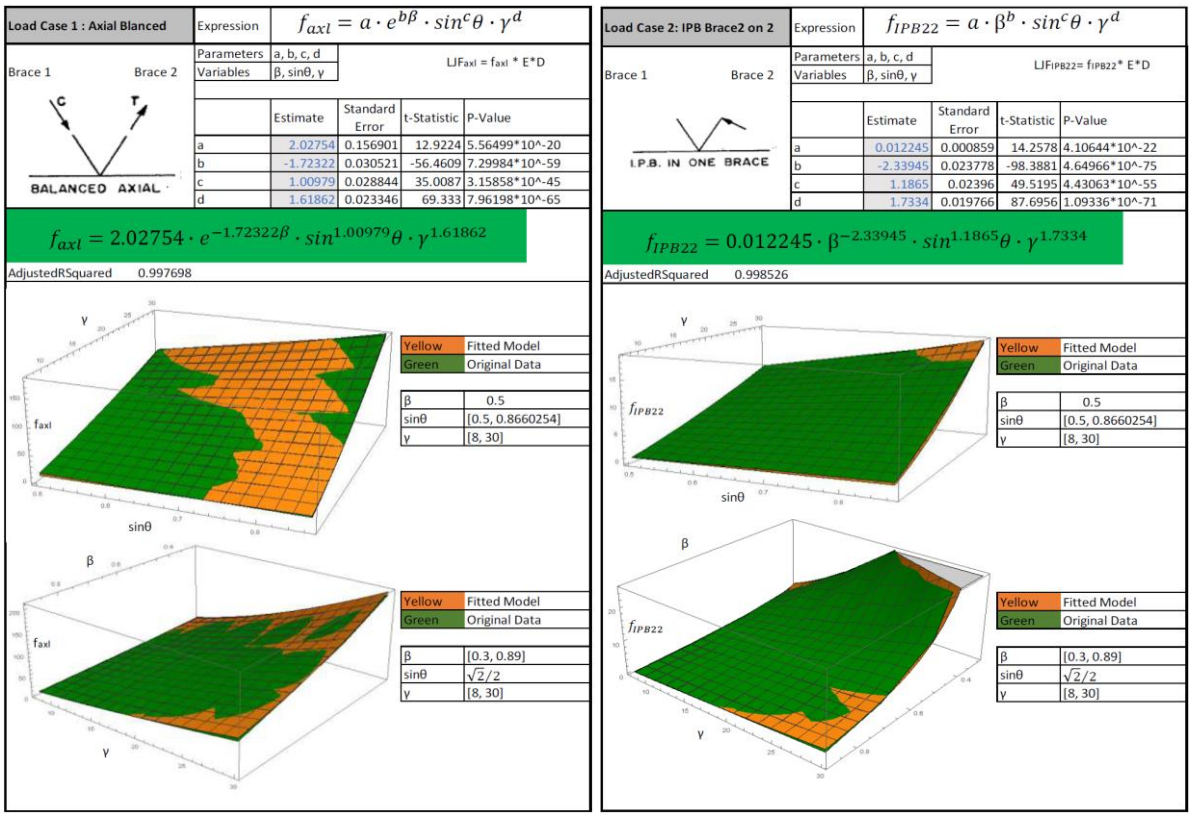

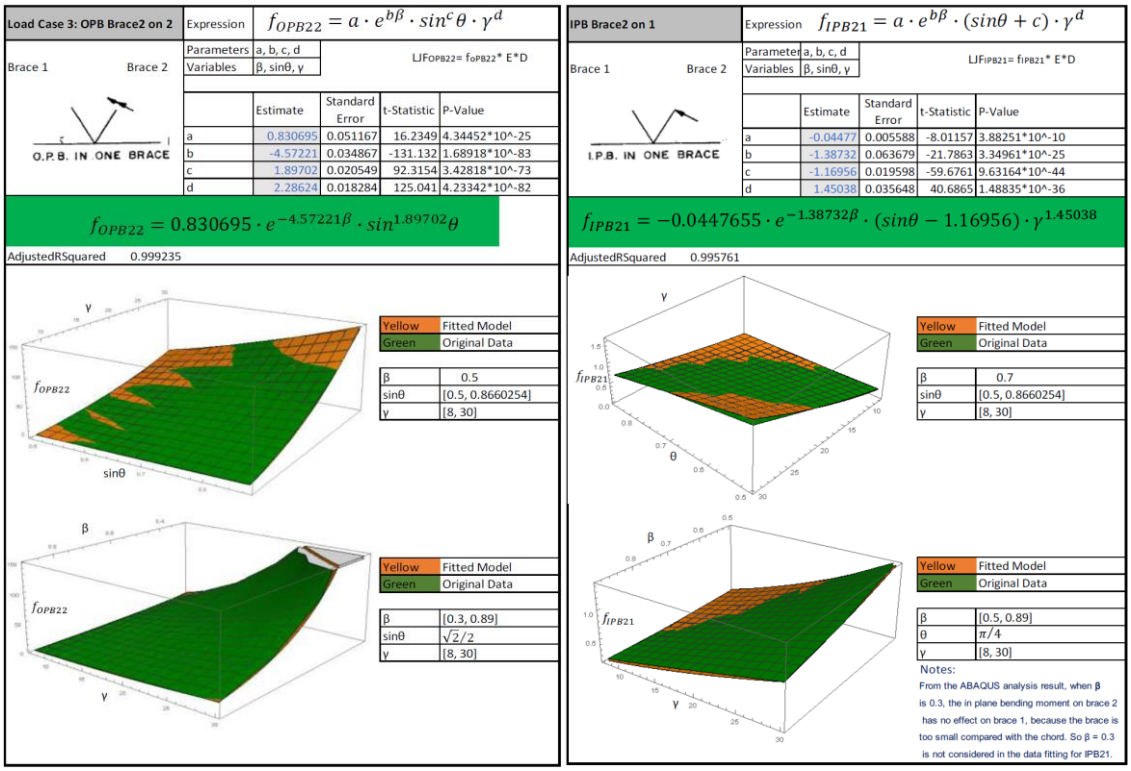

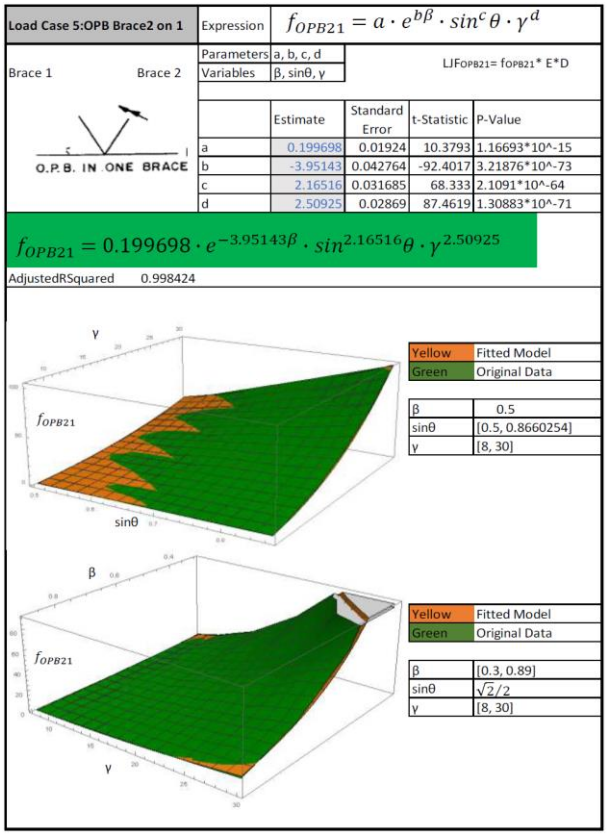

Figure 14 Curve Fitting Exercise in *MATHEMATICA* Software

Condition	RK LJF Parametric Equation	Equation No.
Axially Balanced	$f_{axl} = 2.0275 \cdot e^{-1.7232\beta} \cdot sin^{1.0098}\theta \cdot \gamma^{1.619}$	**(1)**
IPB Brace 2 on 2	$f_{IPB22} = 0.0122 \cdot \beta^{-2.3395} \cdot sin^{1.1865}\theta \cdot \gamma^{1.7334}$	**(2)**
OPB Brace 2 on 2	$f_{OPB2} = 0.8307 \cdot e^{-4.5722\beta} \cdot sin^{1.8970}\theta \cdot \gamma^{2.2862}$	**(3)**
OPB Brace 2 on 1	$f_{OPB21} = 0.1997 \cdot e^{-3.9514\beta} \cdot sin^{2.1652}\theta \cdot \gamma^{2.5093}$	**(4)**
IPB Brace 2 on 1	$f_{IPB2} = -0.04478 \cdot e^{-1.3873\beta} \cdot (sin\theta - 1.1696) \cdot \gamma^{1.4504}$	**(5)**

Table 9 RK-LJF Parametric Equations for Axial, IPB and OPB

9.0 RK-LJF COMPARISON STUDY

A comparison study was performed on the basis of the AMOCO K-Joint Tests for varying β values (β = 0.30, β = 0.50, β = 0.70, β = 0.89) and existing LJF formulations. The AMOCO K-Joint tests are represented below for β = 0.89.

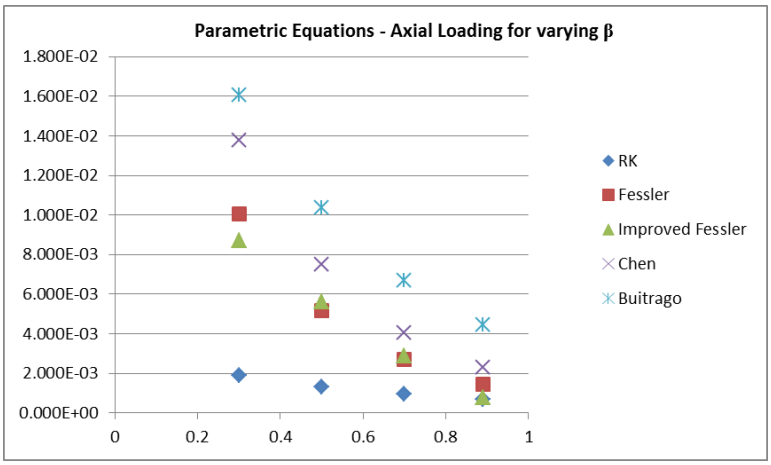

Figure 15 LJF Comparison for Axial loading vs varying β
Note 1: LJF units for Axial Loading: mm/kN

For the axially loaded condition, Figure 15 shows that previous LJF formulations have overestimated these loading effects. For the OPB and IPB conditions (Figure 16 and 17) both cross terms and direct terms have been included. All LJF equations show an increasing trend as β values decreases. This is highly expected with RK-LJF formulations providing more flexibility than the others. It is also important to note that other LJF equations have all been a derivative of each other in terms of the limited and similar database of joints used in the past twenty years.

RK-LJF formulations are based on an up-to-date database of in-service K-type joints. These results must be treated with caution at this stage as the full effects of LJFs are when they are incorporated within a truss framework with re-distribution of moments and loading are considered. The RK-LJF equations will be validated against large scale testing and the MSL equations to show a good agreement for ultimate strength as provided in Section 11.0.

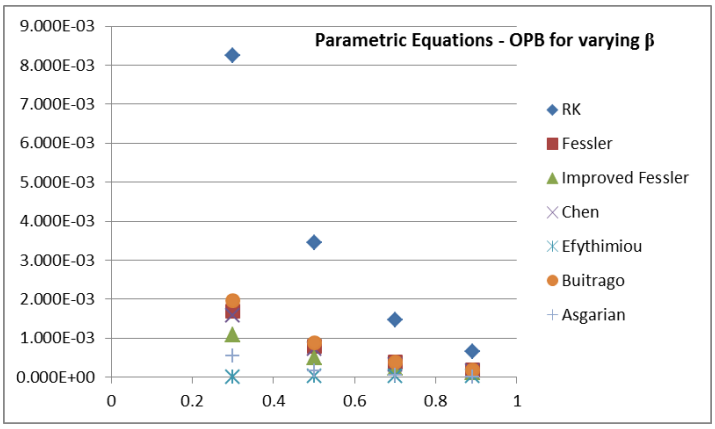

Figure 16 LJF Comparison for OPB vs varying β
Note 2: LJF units for OPB: 1/kN.m

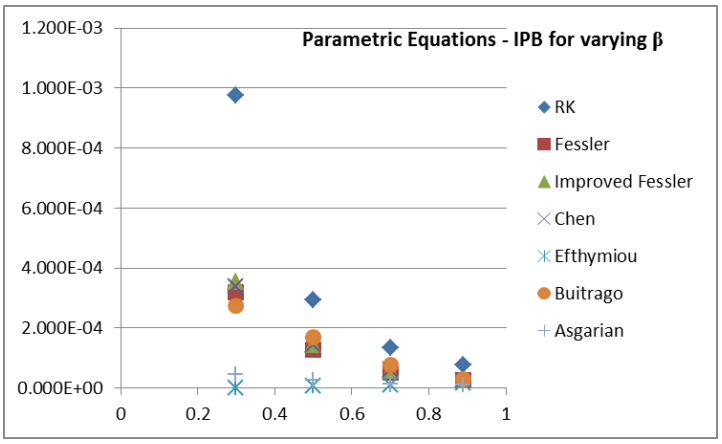

Figure 17 LJF Comparison for IPB vs varying β
Note 3: LJF units for IPB: 1/kN.m

10.0 DEEPER UNDERSTANDING OF THE FATIGUE PHENOMEMA WITH REGARDS TO AGEING OFFHSORE STRUCTURES

Prior to the early 2000s, it was generally accepted that fatigue lives for existing structures was the governing criteria for asset life extension and continuous operations. With MSL Engineering publishing a *JIP Rationalization and Optimization of Underwater Inspection Planning consistent with API RP 2A Section 14* (2000) [18], the general understanding of fatigue as it relates to fixed offshore structures would now be changed. This JIP considered a wide database of in-service structures in the Gulf of Mexico of various vintages to consider various degradation mechanisms. The pre-API structures ranged from 1948 to 1971. As fatigue is a time dependent phenomena, it would be expected that, all things being equal, fatigue cracks would be found in the older structures of the pre-API vintage. Figure 18 shows the contradiction where platforms installed towards the later part of the era show greater susceptibility to fatigue to general fatigue cracking.

For most oil and gas operators, this JIP revealed that the concept of fatigue considerations can be addressed within their Structural Integrity Management System (SIMS). Nichols and Khan (2015) [20] demonstrated that embarking on a Risk Based Underwater Inspection (RBUI) approach, together with a good anomaly management program, and with platform CP functionality, and global ultimate strength assessments on the jacket structures, platforms of all vintages can be managed effectively with limited resources. These practices have now been included in the API RP 2SIM (2014) and the ISO SIM 19901-09 (DIS) and adopted by many leading operators as global standards for managing fixed offshore structures.

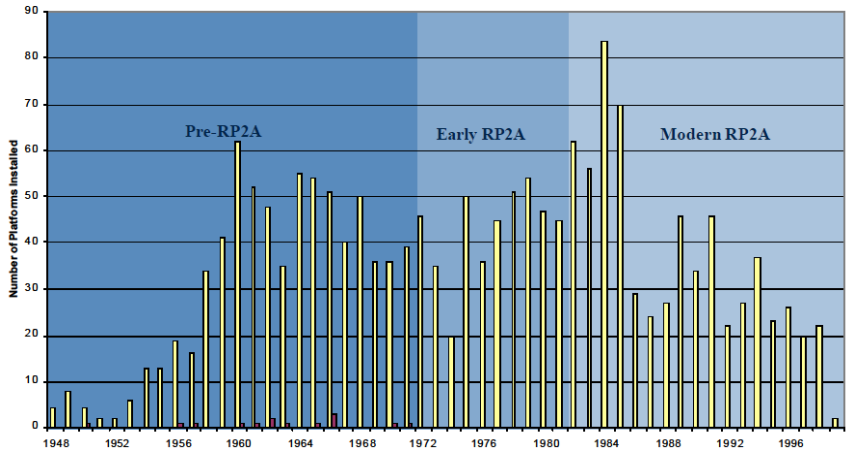

Yellow (longer) bars show number of platforms installed
Red bars show number of platforms with multiple (>1) suspected general fatigue cracks

Figure 18 Pre-API RP 2A Vintage Platforms with multiple fatigue cracks (MSL, 2000)

11.0 VALIDATION OF THE RK-LJF EQUATIONS FOR GLOBAL ASSESSMENTS OF FIXED OFFSHORE STRUCTURES

Since the early and mid-2000s, most of the work on local joint flexibility analyses and parametric equation development by MSL (2002), Miterhari (2009) and Qian et al (2013) have based their research on understanding the effects of LJF on the frame or truss system to represent the jacket template of offshore structures in global ultimate strength assessments. The most noteworthy large scale benchmarking exercise against that has been done was by MSL (1994, 1998) where revised formulations to the MSL-ISO joint strength formulae (2002) were presented. These formulations were then benchmarked against the BOMEL frames test (1995) and provided a set of formulations that considered LJF implicitly.

ISO 19902 (2007) reports that, *"full non-linear deformation curves for joints can be required for pushover analysis to determine a system ultimate strength, especially when joint failures participate in the sequence leading to system collapse. Such pushover analyses are common in studies for maintenance and life extension of structures."* ISO also reports that with the MSL (1994, 1998) work, *"the understanding of linear elastic flexibility has been extended, through the analysis of an updated database and a range of closed-form expressions was established which permit the creation of non-linear load deformation curves in both loading and unloading regimes for simple joints across the practical range of load cases and geometries."*

The results obtained by MSL for their benchmarking working against the BOMEL large scale tests results [4] provide the basis for this validation exercise. The RK-LJF was included in the Frames VII USFOS structural model and the load vs deflection results for the rigid joint, MSL-ISO joint, BOMEL test data and the RK-LJF formulations were compared.

To perform the analysis, the following procedure was followed:

- Create an USFOS model using the BOMEL Frame VII (K-Frame) configuration, material properties and loading mechanisms.
- Use the USFOS pushover module to replicate the P-delta for the test data.

Four cases of analysis were performed, with the flexibility options in Table 10

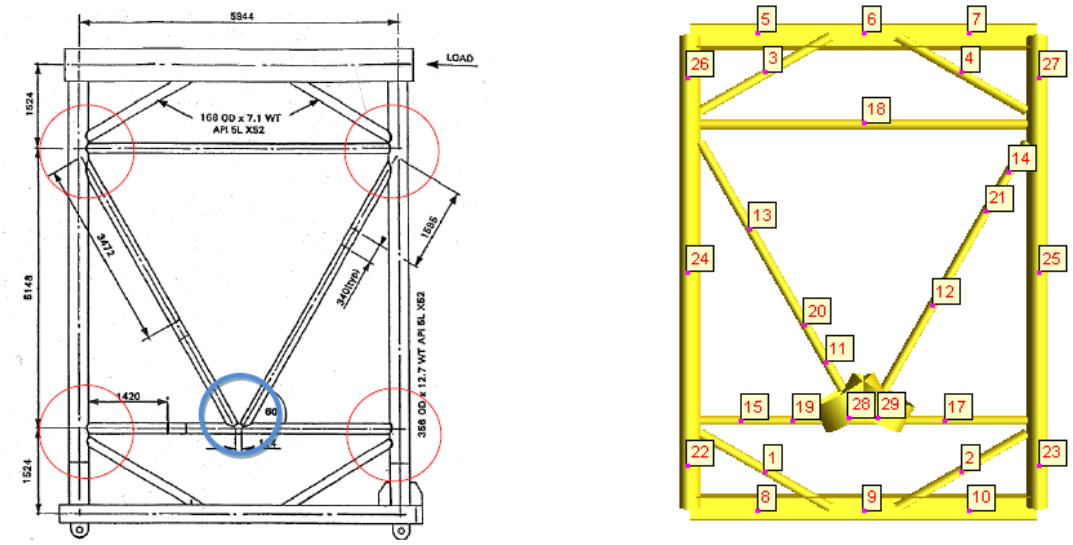

Figure 19 BOMEL Frame Tests modelled in USFOS and including RK-LJF Formulations for K-type joint

Case No.	Joint Flexibility Options	Comments
1	No LJF or joint strength check	Rigid joint analysis
2	USFOS Joint check using MSL-ISO equations	All 5 K-type joints (one circled red and 4 circled blue) on Figure 19
3	USFOS Joint check using MSL-ISO equations	For the K-type joint circled in blue on Figure 19
4	RK-LJF using an updated model to Case 1 by inserting two short stub brace members (circled blue on Figure 19) at center of the frame	The properties for the short stub members were calculated based on the K-joint configuration

Table 10 Joint Flexibility Options for RK 2D Frame validation study

To develop the two short stub brace members to represent the flexible joints, a similar approach is used to the one used by MSL (2001) in *The effects of local joint flexibility on the reliability of fatigue life estimates and inspection planning* [11] for the HSE Executive. The methodology has been tailored to accommodate the element modeling capabilities of the USFOS program. The method involves inserting a short stub flex–element at the end of each brace. The short stub flex-element connects the brace to the chord. RK-LJF formulations give explicit formulae for the various uni-planar K-type joints based on their geometry. The Equations 1-5 (RK-LJF) are employed to calculate the LJF for the joint circled in blue on Figure 19. The result is then used to calculate the necessary area and inertial properties of the flex-element to represent axial, in-plane and out-of-plane bending. The flex-elements are represented as Elements 28 and 29 on Figure 19 (USFOS model).

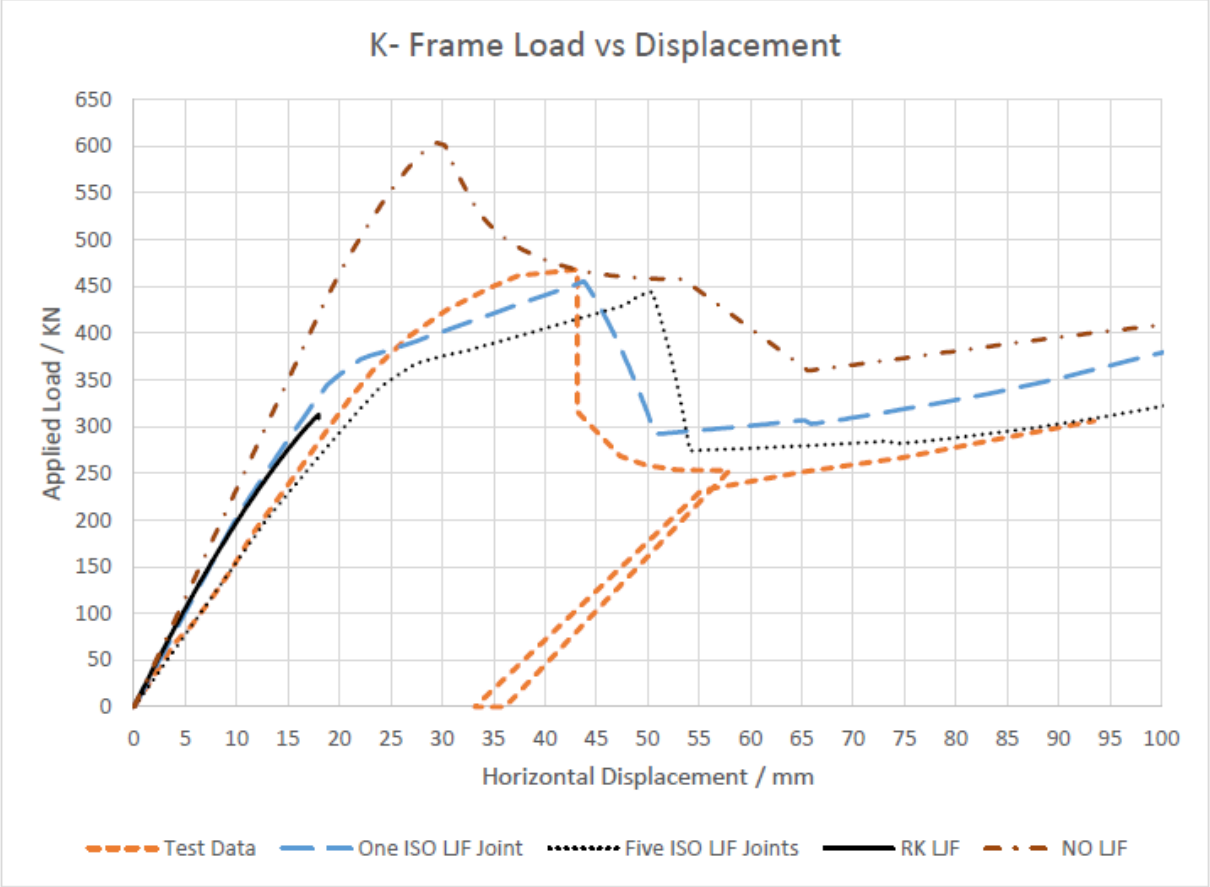

Figure 20 Load vs Displacement Curve (RK-LJF included)

Figure 20 provides the load displacement curves for all four cases outlined in Table 10. If no LJF is included, the structure computer model behaves much stiffer than the prototype test data ie BOMEL large scale tests (compared results from analysis Case 1 with test results). From the BOMEL K-frame prototype tests results, the initial deformation across the compression intersection contributed to the initial softening of the frame response. Before the peak joint load was reached, a crack was initiated at the chord crown weld toe of the tension brace intersection in the gap region. The crack rapidly propagated around the weld toe generating an abrupt and significant reduction in the global load. The analysis results for Case 2 provides a good representation of the test data as the USFOS LJF or joint strength was calibrated against the large scale test data. For the analysis from Case no 3, the results show stiffer than the results from Case 5, LJF joints being modeled (Case 2) but more flexible than the case without LJF (analysis results in Case 1). The analysis results in Case 4 (RK-LJF) are similar to the results achieved from the analysis in Case 3 (MSL-ISO) above, which is expected. The RK-LJF results from this study using ABAQUS result in the frame that is slightly more flexible than the ISO formulation (which is of benefit and closer to the physical prototype model ie the BOMEL test results). The RK-LJF results are within 5% of the prototype tests results but are confined to the linear elastic region, as the RK-FEA benchmarking exercise was performed using linear elastic displacement values and the large scale AMOCO tests were performed in the linear elastic range. There is an opportunity in the future for researchers to develop the RK-LJF equations for the inelastic range of stress.

12.0 CONCLUSIONS

The improved suite of RK LJF formulations (Eq 1-5) has been developed to represent a full geometric range of in-service K-type single planar joints. The formulations were developed by benchmarking a finite element tubular joint model to the AMOCO K-Joint Test results (the only large scale measurement of LJF performed) and then adopting the approach of developing LJFs from the benchmarked model for all geometric ranges of single planar K-Joints. Through studies it is shown that the RK LJF equations show the closest agreement to large scale test results compared to the oft-used MSL-ISO equations in ISO 19902, for uni-planar K-type tubular joints and represents an improvement on current methods.

ACKNOWLEDGEMENTS

The authors of this paper will like to thank Mr Patrick O Connor formerly Global Head of Structural Engineering at BP and Dr Kaisheng Chen for their kind advice throughout the development of this study.

REFERENCES

1. ABAQUS Theory Manual. ABAQUS Suite of Documents, 2011.
2. API Recommended Practice for the *Planning, Designing and Constructing Fixed Offshore Platforms.* (2000) API RP2A. American Petroleum Institute. 22nd Edition.
3. Asgarian B et al (2014). *Local Joint Flexibility Equations for Y-T and K-type Tubular Joints.* Ocean Systems Engineering. Vol 4, No 2 (2014). 151-167
4. Bolt, H.M. (1995). *Results from Large Scale Ultimate Strength Tests of K-Braced Jacket Frame Structures,* OTC Paper 7783. Offshore Technological Conference, Houston, May 95.
5. Buitrago, J., Healy, B. E. and Chang, T.Y. (1993) *Local joint flexibility of tubular joints,* Offshore Mechanics and Arctic Engineering Conference, OMAE, Glasgow.
6. Chen, B., Hu, Y., and Tan, M., (1990) *Local Joint Flexibility of Tubular Joints of Offshore Structures,* Marine Structures, Vol. 3, pp. 177-197.
7. Da Silva, E.C. (2015). *Fatigue Life of Fixed Offshore Structures according to SCF and LJF Parameters.* MSc Thesis. London South Bank University.
8. Dier, A.F., Hellan, O. (2002). *A non-linear tubular joint response for pushover analysis*. Proceedings of OMAE 2002-28634. 21st International Conference on Offshore Mechanics and Arctic Engineering.
9. DNV *Rules for the Design, Construction and Inspection of Offshore Structures* (1977). Det Norske Veritas
10. DNV Recommended Practice DNV-RP- C203. *Fatigue Design of Offshore Steel Structures.* (2010). Det Norske Veritas
11. *Effects of local joint flexibility on the reliability of fatigue life estimates and inspection planning* Health and Safety Executive. Offshore Technological Report 2001/056, 2001
12. Efthymou, M. (1985) *Local rotational stiffness of unstiffened tubular joints,* Shell Report (KSEPL) RKER.85.199.
13. Fessler H, Mockford P.B. and Webster J.J. (1986) *Parametric Equations for the flexibility matrices of multi-braced tubular joints in offshore structures.* Proceedings to the Institution of Civil Engineers. Part 2. 1986. 81. Dec. 675- 696. Paper 9124.
14. Fessler H, Mockford P.B. and Webster J.J. (1986) *Parametric Equations for the flexibility matrices of single-braced tubular joints in offshore structures.* Proceedings to the Institution of Civil Engineers. Part 2. 1986. 81. Dec. 679- 673. Paper 9089.
15. Hoshyari, I and Kohoutek, R (1993). *Rotational and axial flexibility of tubular T-joints.* Offshore and Polar Engineering Conference ISOPE, Singapore.
16. ISO 19902: 2007 *Fixed Steel Offshore Structures* British Standards International. 2007. 1st Edition.
17. Leman 49/27AD. K-Joint Tests (1983). *Final Report. Amoco (UK) Exploration Co. Report No ST 102/83A.* May 1983.
18. MSL Engineering Ltd. *JIP Rationalization and Optimization of Underwater Inspection Planning consistent with API RP 2A Section 14* (2000).
19. Nichols, N.W. et al (2006). *Managing Structural Integrity for Ageing Platform.* SPE-101000-PP.
20. Nichols, N.W and Khan, R (2015). *Structural Integrity Management System (SIMS) Implementation within PETRONAS' Operations*. Journal of Marine Engineering & Technology. Volume 14. Issue 2.

21. O'Connor .P, Bucknell J., Westlake HS, Puskar F. (2005). *Structural Integrity Management (SIM) of Offshore Facilities.* Offshore Technological Conference, Paper 17545.
22. Qian X et al (2013). *A Load-Deformation Formulation for CHS X and K-Joints in Pushover Analysis.* Journal of Constructional Steel Research 90 (2013). 108-119.
23. Romeijn, A., Puthli, R. S., and Wardenier, J., *Finite Element Modeling of Multi-planar Joint Flexibility in Tubular Structures,* Proceedings of the Second International Offshore and Polar Engineering Conference, Vol. IV, International Society of Offshore and Polar Engineers, pp. 420-429, 1992.
24. Ueda, Y., Rashed, S. M. H., and Nakacho, K.,(1990) *An Improved Joint Model and Equations for Flexibility of Tubular Joints,* Journal of Offshore Mechanics and Arctic Engineering, vol. 112, pp. 157-168, 1990..